

Reduced muscle contraction and a relaxed posture during sleep-like Lethargus

Juliane Schwarz, Jan-Philipp Spies and Henrik Bringmann*

Max Planck Institute for Biophysical Chemistry; Göttingen, Germany

Keywords: Lethargus, sleep, posture, muscle, calcium, GCaMP

Sleep is characterized by reduced muscle activity resulting in reduced movement and a typical posture compatible with relaxed muscles. Prior to each molt, *C. elegans* larvae go through a phase of behavioral quiescence called Lethargus. Lethargus has sleep-like properties, but a specific posture has not yet been described. Do *C. elegans* larvae relax their muscles during sleep and do they assume a typical posture? We measured worm posture and body wall muscle activity using calcium imaging across the sleep-wake-like cycle. We found that worms were less curved and had less muscle activity during the sleep-like state. We conclude that during Lethargus, muscle activity is reduced, resulting in a relaxed body posture typical for a sleep-like state.

Sleep-like states occur in the lives of all animals carefully studied. Sleep-like states are defined by an increased arousal threshold, reversibility, homeostasis, reduced movement, and a typical body posture.^{1,2} Whereas wake postures are often supported by skeletal muscle, sleep postures need to be compatible with relaxed body muscles. Typically, sleep postures fit the substrate the animal is sleeping on.² As a result, sleep postures are species-specific and variable. In mammals, the electromyogram is often used to measure muscle relaxation during sleep.³ Muscle contraction is caused by cytosolic calcium and genetically encoded fluorescent calcium sensors can be used to measure muscle calcium and thus muscle activity.⁴ *C. elegans* larvae proceed through four larval stages until they reach adulthood. At the end of each stage, worms molt. Prior to ecdysis, worms display a behavioral quiescence called Lethargus,⁵ which has sleep-like properties, such as an increased arousal threshold, reversibility, and homeostasis.⁶ However, a sleep-specific posture or reduced muscle calcium have not been described. Here we show that *C. elegans* has reduced muscle activity during Lethargus and assumes a relaxed posture during this sleep-like state.

We wanted to know whether *C. elegans* larvae relax their muscles and assume a sleep-specific posture during Lethargus. We generated transgenic worms expressing the calcium sensor GCaMP3.35 in striated body wall muscles.^{7,8} We cultured larval worms inside agarose hydrogel microcompartments from the first to the second larval stage.⁹ Every ten minutes, we measured movement, posture, and muscle calcium. To do this, we first filmed worms using bright-field imaging to identify the non-pumping phase. Then, widefield fluorescence images were taken to record movement, worm shape and calcium sensor intensities

(Fig. 1A). We identified sleep-like states based on feeding activity and nose speed. During the non-feeding phase, worms movement was lowered by 79% (Mean nose speed wake-like state: $12.1 \pm 0.6 \mu\text{m/s}$, sleep-like state: $2.7 \pm 0.3 \mu\text{m/s}$, $p < 0.001$, $n = 15$ worms; Figure 1B). *C. elegans* moves in a sinusoidal locomotive pattern and typically assumes a curved posture.¹⁰ The curvature of the worm can be quantified by measuring the angle change between consecutive linear segments fitted along the axis of the worm.^{11,13} We found that the angle change was 19.5% less during the sleep-like state in comparison to the wake-like state (angle change wake-like state: 0.193 ± 0.005 rad, sleep-like state: 0.165 ± 0.008 rad, $p < 0.001$, $n = 15$ worms; Figure 1C).

We then used GCaMP3.35 imaging to measure muscle activity. A basal GCaMP3.35 signal was always visible in all body wall muscles. In the wake-like state, some body wall muscle areas showed a strong increase (about 65%) in GCaMP3.35 intensity. These areas of increased intensity usually occurred at the contracting side of a body bend. During the sleep-like state, local GCaMP3.35 increases were rare and the GCaMP3.35 signal appeared more even along the body wall muscles (Fig. 1A). The overall GCaMP3.35 signal increased linearly over time along with the growth of the animal. However, during the sleep-like state, the GCaMP3.35 signal declined by 9% (GCaMP3.35 intensity wake-like state: 1090 ± 44 , sleep-like state: 991 ± 43 , $p < 0.001$, $n = 15$ worms; Figure 1D). Taken together, these results show that *C. elegans* larvae relax their body wall muscles during sleep-like Lethargus resulting in a less curved posture typical for the sleep-like state. Because a sleep-specific posture is a defining criterion for sleep-like states² this result corroborates the idea that Lethargus is a sleep-like state.

*Correspondence to: Henrik Bringmann; Email: Henrik.Bringmann@mpibpc.mpg.de
Submitted: 11/07/11; Revised: 01/19/12; Accepted: 01/26/11
<http://dx.doi.org/10.4161/worm.1.1.19499>

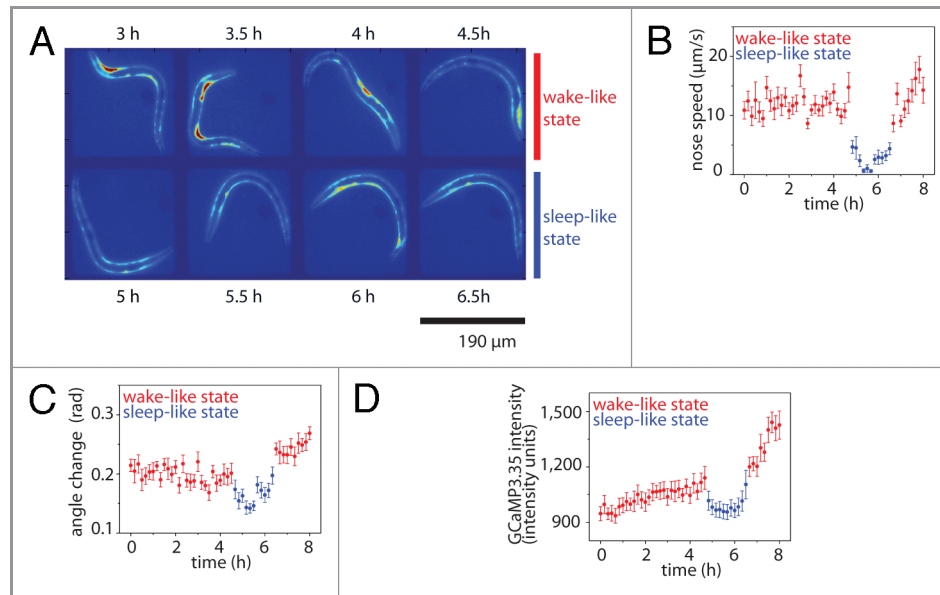


Figure 1. Reduced movement, body curvature, and muscle activity during sleep-like Lethargus. **A** Time-lapse images showing the microcompartment including the entire worm during wake-like state (top) and sleep-like state (bottom). The bright signal is derived from the body wall muscle and reflects calcium intensities. **B** Motility is reduced during *C. elegans* sleep-like state. We measured averaged nose speed. **C** Reduced curvature during *C. elegans* sleep-like state. We measured angle change along the long axis of the worm. **D** Reduced muscle activity during *C. elegans* sleep-like state. We measured GCaMP3.35 intensity. Error bars are SEM $n = 15$ worms. In the plots, wake-like state is colored red and sleep-like state is colored blue. Individual worms were aligned by the start of Lethargus as defined by cessation of pumping.

Experimental Methods

Strains and worm maintenance. *C. elegans* was maintained on NGM plates as described.¹² The following strain was used:

HBR4; *goels3[pmyo-3::GCaMP3.35::unc-54-3'utr, unc-119(+)]V*.

GCaMP3.35 calcium indicator. We used the green fluorescent protein calcium indicator GCaMP3.35 as described previously.⁸

Imaging and image analysis. Worms were cultured in hydrogel agarose microcompartments.⁹ Imaging was performed on a Nikon TiE microscope equipped with hardware autofocus (Perfect Focus System). XY scans were performed with a Prior Scientific Proscan Stage. For fluorescence microscopy, samples were illuminated with LED (490nm, CoolLED) and imaged with standard light filters (Chroma or Semrock). Images were acquired using an iXon Camera (Andor). Camera and microscope were controlled with iQ software (Andor). Muscle activity was measured at an interval of 10 minutes. Measurement consisted of first a brightfield movie to see pumping. Then 30 pictures at an interval of 200 ms were taken to measure GCaMP3.35 fluorescence. Nose speed was measured manually at an interval of one second and was averaged for each time point. We determined mean intensity of GCaMP3.35 and angle change at every time point.

Angle change. We used a semiautomatic method for determination of the midline of the worm from fluorescence images. Automatic determination of the skeleton: To extract the midline automatically, the outline of the nematode was determined using a “Canny-Edge” algorithm.¹³ We used parameters as follows:

$\sigma = 3\text{px}$, $T1 = 0.03$; $T2 = 0.2$. Edge segments shorter than five pixels or corresponding to the border of the microcompartment were discarded using a custom written program. We dilated the obtained outline by a spherical element of 20 pixels diameter and used a thinning operation to obtain the midline. We manually checked that the midline was correctly identified. In 26% of the images the algorithm did not produce a correct result. This mainly occurred when the worm was touching itself. If the result was not correct we manually determined the midline: We manually placed 20 to 30 points along the midline of the worm using a custom written MATLAB routine that recorded the position of mouse clicks on a fluorescence image. We then identified intermediate pixel positions linking the clicked points linearly using the Bresenham’s line algorithm.¹⁴ Angle change along the midline of the nematode was computed using a custom MATLAB routine that divided the midline into 20 equal segments. Then, the routine approximated each segment by a line linking its endpoints to obtain a polygonal chain, and calculated the local angle change Θ_i between two consecutive segments as $\Theta_i = \arctan((y_{i+2}-y_{i+1})/(x_{i+2}-x_{i+1})) - \arctan((y_{i+1}-y_i)/(x_{i+1}-x_i))$, with x_i, y_i : pixel values of beginning of i^{th} line segment. The angle change for one polygonal chain was defined as the mean value of the local angle change values Θ_i : $\Theta = \text{mean}(\Theta_i)$.

Statistical tests and data display. For each worm, all data points during the sleep-like state were averaged and 15 time points before the sleep-like state were averaged. For all statistical tests, Wilcoxon Signed Rank Tests were performed using Origin software. For displaying the micrograph we applied false colors to the grayscale image with the standard color map “jet” in Matlab.

Acknowledgments

We thank E. Friedhoff for help with manual data processing and S. Ernst for bombardment.

References

1. Campbell SS, Tobler I. Animal sleep: a review of sleep duration across phylogeny. *Neurosci Biobehav Rev* 1984; 8:269-300; PMID:6504414; [http://dx.doi.org/10.1016/0149-7634\(84\)90054-X](http://dx.doi.org/10.1016/0149-7634(84)90054-X)
2. Hendricks JC, Sehgal A, Pack AI. The need for a simple animal model to understand sleep. *Prog Neurobiol* 2000; 61:339-51; PMID:10727779; [http://dx.doi.org/10.1016/S0301-0082\(99\)00048-9](http://dx.doi.org/10.1016/S0301-0082(99)00048-9)
3. Jacobson A, Kales A, Lehmann D, Hoedemaker FS. Muscle Tonus in Human Subjects during Sleep and Dreaming. *Exp Neurol* 1964; 10:418-24; PMID:14228400; [http://dx.doi.org/10.1016/0014-4886\(64\)90033-0](http://dx.doi.org/10.1016/0014-4886(64)90033-0)
4. Kerr R, Lev-Ram V, Baird G, Vincent P, Tsien RY, Schafer WR. Optical Imaging of Calcium Transients in Neurons and Pharyngeal Muscle of *C. elegans*. *Neuron* 2000; 26:583-594; PMID:10896155; [http://dx.doi.org/10.1016/S0896-6273\(00\)81196-4](http://dx.doi.org/10.1016/S0896-6273(00)81196-4)
5. Cassada RC, Russell RL. The dauerlarva, a post-embryonic developmental variant of the nematode *Caenorhabditis elegans*. *Dev Biol* 1975; 46:326-42; PMID:1183723; [http://dx.doi.org/10.1016/0012-1606\(75\)90109-8](http://dx.doi.org/10.1016/0012-1606(75)90109-8)
6. Raizen DM, Zimmerman JE, Maycock MH, Ta UD, You YJ, Sundaram MV, et al. Lethargus is a *Caenorhabditis elegans* sleep-like state. *Nature* 2008; 451:569-72; PMID:18185515; <http://dx.doi.org/10.1038/nature06535>
7. Tian L, Hires SA, Mao T, Huber D, Chiappe ME, Chalasani SH, et al. Imaging neural activity in worms, flies and mice with improved GCaMP calcium indicators. *Nat Methods* 2009; 6:875-81; PMID:19898485; <http://dx.doi.org/10.1038/nmeth.1398>
8. Schwarz J, Lewandrowski I, Bringmann H. Reduced activity of a sensory neuron during a *C. elegans* sleep-like state. *Curr Biol* (. In press. PMID:22192827
9. Bringmann H. Agarose hydrogel microcompartments for imaging sleep- and wake-like behavior and nervous system development in *Caenorhabditis elegans* larvae. *J Neurosci Methods* 2011; 201:78-88; PMID:21801751; <http://dx.doi.org/10.1016/j.jneumeth.2011.07.013>
10. White JG, Southgate E, Thomson JN, Brenner S. The structure of the ventral nerve cord of *Caenorhabditis elegans*. *Philos Trans R Soc Lond B Biol Sci* 1976; 275:327-48; PMID:8806; <http://dx.doi.org/10.1098/rstb.1976.0086>
11. Baek J-H, Cosman P, Feng Z, Silver J, Schafer WR. Using machine vision to analyze and classify *Caenorhabditis elegans* behavioral phenotypes quantitatively. *J Neurosci Methods* 2002; 118:9-21; PMID:12191753; [http://dx.doi.org/10.1016/S0165-0270\(02\)00117-6](http://dx.doi.org/10.1016/S0165-0270(02)00117-6)
12. Brenner S. The genetics of *Caenorhabditis elegans*. *Genetics* 1974; 77:71-94; PMID:4366476
13. Canny J. A computational approach to edge detection. *IEEE Trans Pattern Anal Mach Intell* 1986; 8:679-98; PMID:21869365; <http://dx.doi.org/10.1109/TPAMI.1986.4767851>
14. Bresenham JE. Algorithm for Computer Control of a Digital Plotter. *IBM Syst J* 1965; 4:25-30; <http://dx.doi.org/10.1147/sj.41.0025>

© 2012 Landes Bioscience.

Do not distribute.